Forecast photovoltaic and crop photosynthesis output under solar spectrum shifts from climate change

Geoffrey S. Kinsey
Zuva Energy

Abstract

Greenhouse gases and aerosols in the atmosphere alter the spectrum of sunlight that reaches the Earth's surface. To forecast the effects on photovoltaics and crop photosynthesis, atmospheric parameters from five climate models in the Coupled Model Intercomparison Project (CMIP) were input into the radiative transfer model SMARTS to generate representative spectra over six decades (2018-2082). Geographic and temporal variation was then forecast for the spectral responses of one-, two- and three-junction photovoltaic cells, and three crop plants: corn, wheat, and rice. Results for photovoltaics show baseline (2020) global outputs lower than for the standard spectrum, particularly for solar cells with more than one junction. In the decades ahead, photovoltaic output is forecast to decline due to increased water vapor absorption, while crop photosynthesis is largely unaffected. For both photovoltaics and crop photosynthesis, forecast long-term decreases in atmospheric aerosols lead to net production increases over most of the globe.

Introduction

Humanity converts sunlight into usable energy directly, via solar photovoltaics (PV), and indirectly, via photosynthesis of crop plants. The efficiency of these conversions is dependent on a surface-level sunlight spectrum that is evolving due to climate change. As sunlight passes through the Earth's atmosphere to the surface, the spectrum is absorbed and scattered by gas molecules and aerosols. As greenhouse gases accumulate, radiative forcing increases, resulting in ongoing modification of atmospheric gases and aerosol levels. Alterations in the spectrum of radiation reaching the Earth's surface vary with geographic location and over time. To model surface-level spectrum, atmospheric parameters from five climate models from the Coupled Model Intercomparison Project were input into the radiative transfer model SMARTS to forecast solar spectrum shifts over six decades (2018-2082). The resulting geographic and temporal variation of photovoltaic and photosynthetic output was forecast using the spectral responses of one-, two- and three-junction photovoltaic cells, and three crop plants: corn, wheat, and rice.

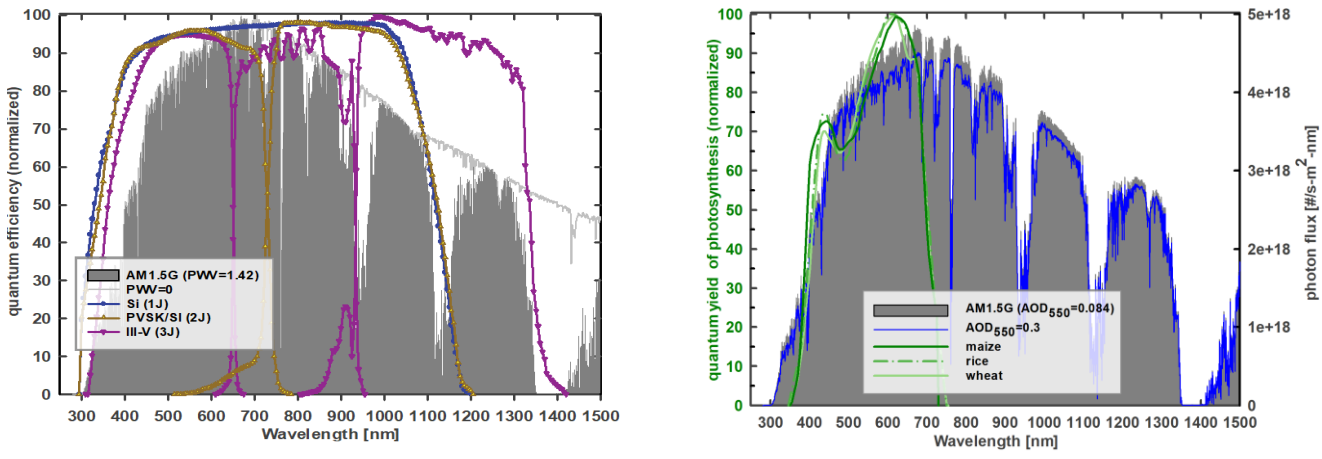

(a) (b)

Figure 1. (a) Quantum efficiencies of single-junction (1J) silicon (Si), tandem (2J) perovskite-silicon (PVSK/Si), and three-junction (3J) III-V multijunction cells[1–3]. The standard terrestrial solar spectrum (AM1.5G) is shown against a spectrum for which the precipitable water vapor (PWV) has been reduced from the standard 1.42 [g/cm^2] to zero.

(b) Spectra of quantum yield of photosynthesis for maize, wheat, and rice[4] shown against the standard terrestrial solar spectrum (AM1.5G) and a spectrum for which the aerosol optical depth at 550 nm (AOD_{550}) has been raised from the standard 0.084 to 0.3.

The atmosphere scatters and absorbs incoming solar radiation. Molecular scattering by oxygen and nitrogen gives us our blue skies and the diffuse component of solar irradiance at the surface. Proportional to the inverse fourth power of the wavelength[5], molecular scattering depends on the density of the air column that the sun's rays pass through. The value may be derived from surface atmospheric pressure, which rises with temperature. Suspended aerosols (particle and liquid) both scatter and absorb radiation. Prehistoric drivers of aerosol levels include forest fires, windborne desert dust and ocean salt, and volcanism. Since the Industrial Revolution,

combustion of fossil fuels has been contributing additional man-made aerosols, including sulfates, nitrates, and carbon.

The roles of water vapor and carbon dioxide in absorbing sunlight and thereby altering the climate (radiative forcing) have been recognized since Eunice Foote's groundbreaking demonstrations in 1856[6]. As climate change accelerates, the radiation trapped by greenhouse gases initiates feedback loops that are altering the composition of the atmosphere that does the trapping[7]. The increase in global mean temperature[8] delivers a rising accumulation of water vapor in the atmosphere, due to elevated ocean and air temperatures that, respectively, increase evaporation rates and the atmosphere's ability to retain the evaporated water.

The trends for future aerosol levels are harder to predict. Burning of fossil fuels produces a range of aerosols, including small particles of sulfates and carbon, which can persist in the upper atmosphere until they form the nucleation site for water droplets and are removed via precipitation. A global transition towards cleaner fuels, if sustained, would decrease these levels, but the rate at which various countries will pursue this transition is uncertain[9]. Local differences in future aerosol levels also arise from changes in regional wind speeds that are occurring as the planet warms and wind patterns shift[10]. The distribution of aerosol levels from natural and manmade sources will therefore remain heterogeneous across the planet[11]. Temperature changes from the scattering and absorption of sunlight by these localized aerosols lead to fluctuations in rates of evaporation, cloud formation, and precipitation, as well as a host of other feedbacks that will alter regional and global weather patterns[7].

Efforts to measure and model such trends, and their interactions, span more than a century[12]. Foote's experiments in the mid-1800s provided an answer to the mystery that had surrounded evidence of ancient temperature oscillations being revealed in the geological record[13]. Decades later, climate modeling had its beginnings in weather modeling, which first incorporated atmospheric circulation (1955) and then coupled it with oceanic circulations in the 1960s[14]. The Coupled Model Intercomparison Project (CMIP) was established in 1995 to improve model accuracy and provide a shared knowledge base to inform international action to mitigate climate change. The sixth iteration (CMIP6)[15] began in 2013 and comprises 23 models which provide the underlying data for the multi-decade forecasts in reports by the Intergovernmental Panel on Climate Change (IPCC)[16]. Various future scenarios (Shared Socioeconomic Pathways, SSPs) are evaluated based on the expected level of radiative forcing from additional solar radiation being retained in the atmosphere, land, and water. The scenarios are numbered sequentially by the expected radiative forcing by 2100: scenario 1 assumes aggressive carbon reduction and low radiative forcing of 1.9 W/m^2 (SSP119); with continued expansion of fossil-fuel combustion, scenario 5 expects forcing to reach 8.5 W/m^2 by 2100 (SSP585). An intermediate condition considered here is scenario 2: 4.5 W/m^2 (SSP245).

The effects of climate change on photovoltaics due to alterations in temperature, broadband irradiance, and cloud cover, have been studied previously[17–35]. Analysis of (broadband) shortwave radiation from CMIP5 models has shown that PV production in Europe increases in summer and decreases in winter[36]. To isolate the additional impact of spectrum variation[37], results here are taken at 25° C and normalized to the broadband irradiances. Clear sky conditions are assumed.

The rate of photosynthesis is a primary factor in crop yield[38]. Changes in the available spectrum affect leaf morphology and the resulting rate of photosynthesis[39]; attention to the spectrum of light is a key condition for productive growth under artificial lighting, for example[40,41]. The quantum yield of photosynthesis provides a prediction of the crop growth rates that result when water, nutrient, and temperature conditions are sufficient to give growth that becomes limited by the available sunlight. Slowing of the rate of photosynthesis due to deficits in the solar spectrum can then reduce outdoor crop yields by extending the time to harvest and thereby increasing the risk of exposure of a crop to droughts, floods, and pests.

Methods

CMIP6 models produce over a thousand parameters for changes to the geosphere. The parameters of interest here are those used by the radiative transfer model SMARTS to generate representative solar spectra at the Earth's surface[37]. The SMARTS model is widely used in photovoltaics for its ability to calculate the spectra incident on tilted surfaces, and to define reference spectra[42]. Parameters used for generating spectra in SMARTS are: aerosol optical depth at 550 nm (AOD, Figure 5), carbon dioxide, relative humidity, ozone, precipitable water

(Figure 3), surface pressure (Figure 10), surface air temperature, and surface maximum temperature (Figure 11). Inputs were drawn from five CMIP6 models: ESM2-1[43,44] (National Centre for Meteorological Research, "CNRM"), UKESM1-0-LL[45,46] (Met Office Hadley Center, "MOHC"), ES2L[47,48] (Japan Agency for Marine-Earth Science and Technology, Centre for Climate System Research / National Institute for Environmental Studies "MIROC"), GISS-E2-1-G[49,50] (National Aeronautics and Space Administration, "NASA"), and GFDL-ESM4[51,52] (National Oceanic and Atmospheric Administration, "NOAA"). Data was sampled at monthly intervals.

For forecasting solar cell performance, the spectra generated by SMARTS combined with the quantum efficiency (Figure 1a) of the solar cell gives the predicted short-circuit current[53–56]. Representative quantum efficiencies were from recent-best laboratory cells[1]. An analogous process was used for crop plants, using the relative spectra of quantum yield of photosynthesis[4] (Figure 1b).

2020 baseline: comparison with the PV standard spectrum

Using 2020 as a baseline year, the geographic distribution of photovoltaic output can be compared against that under a standard reference spectrum (AM1.5G). Results for the three solar cell designs are shown in Figure 2Figure 1. Except for silicon solar cells in the northern hemisphere in winter, the modeled spectra indicate lower output than under this standard spectrum. Lower performance of silicon in the southern hemisphere, and the generally lower performance for 2- and 3-junction designs, is consistent with measured results[56].

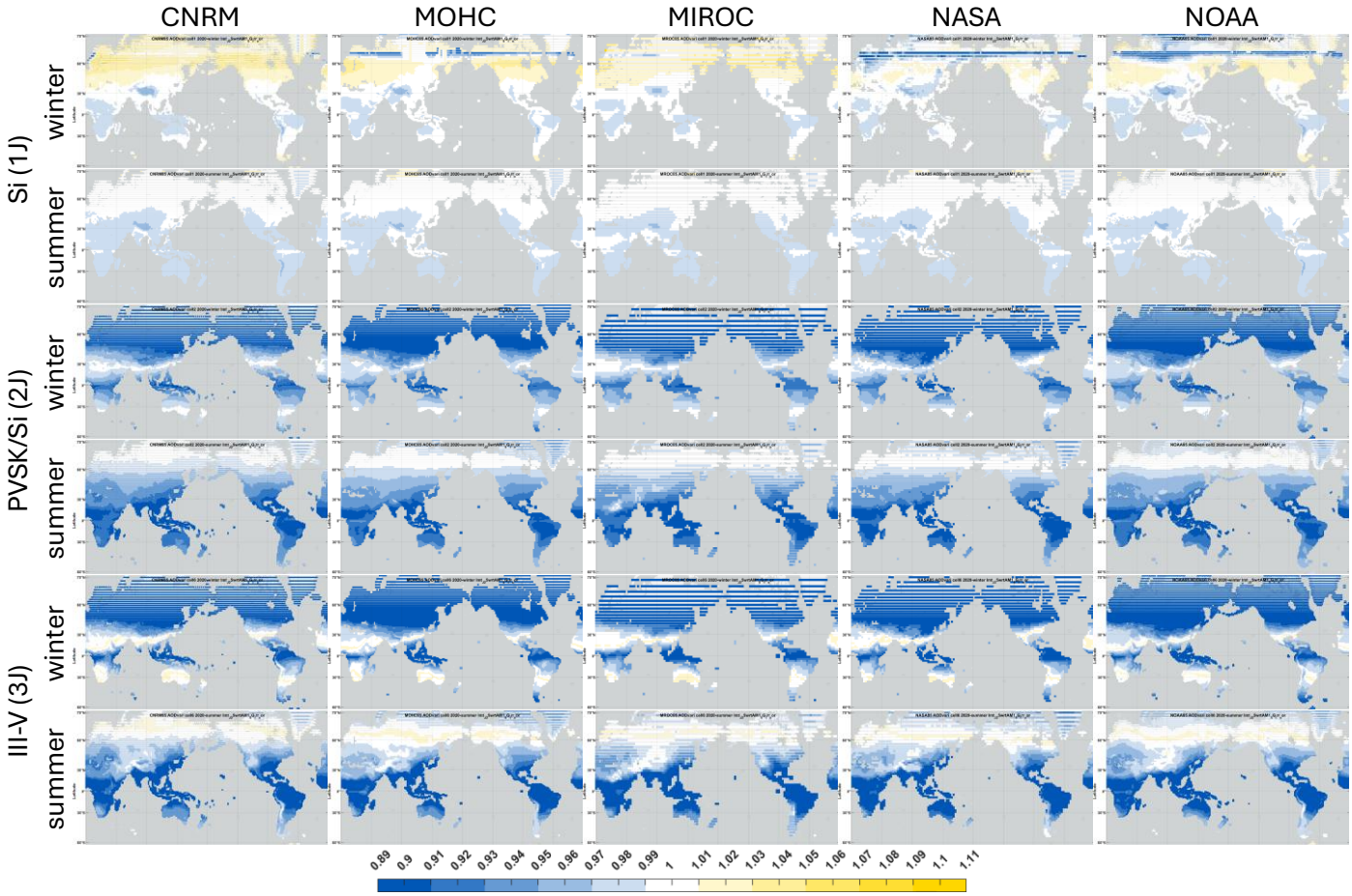

Figure 2. Predicted 2020 solar cell short-circuit current relative to that under the standard spectrum (AM1.5G) at 25° C (scenario: SSP585). Currents are normalized to 1000 W/m² irradiance. "Summer"/ "winter" corresponds to months 6-8/12-2 in the northern hemisphere and 12-2/6-8 in the southern hemisphere.

The widespread use of photovoltaics as an energy source means that even single-digit percent changes translate to large economic impacts. Approximately 760 GW of PV was operating worldwide in 2020[57], so (assuming 1500 kWh of generation per kW of capacity) a 1% increase/decrease in Figure 2 equates to 11 TWh of generation gained/lost; equivalent to the annual total electricity consumption of Lithuania[58].

For solar cells with more than one junction, series connection of the sub-cells means that the output current is limited by whichever junction is producing the least. The resulting increase in spectrum sensitivity makes analyses using a single spectrum less predictive of operating efficiency and insufficient for comparing cells with different spectrum sensitivities[53,54,56]. This is evident in Figure 2 for the two-junction (2J) perovskite-silicon and

the three-junction (3J) III-V multijunction cells, with nominally higher efficiencies (measured with the standard spectrum), but for which the predicted output is often more than 5% lower than for silicon in tropical latitudes in summer and temperate latitudes in winter. The lower performance highlights the limitations of relying on a single standard spectrum for PV analysis. While solar technologies are usually evaluated using ranges for temperature and broadband irradiance, the habit of evaluating PV with just a single standard spectrum remains commonplace in both photovoltaic development and deployments. As with temperature and broadband irradiance, evaluations under more than the one spectrum condition would better inform design optimization and reduce forecast errors[53,56].

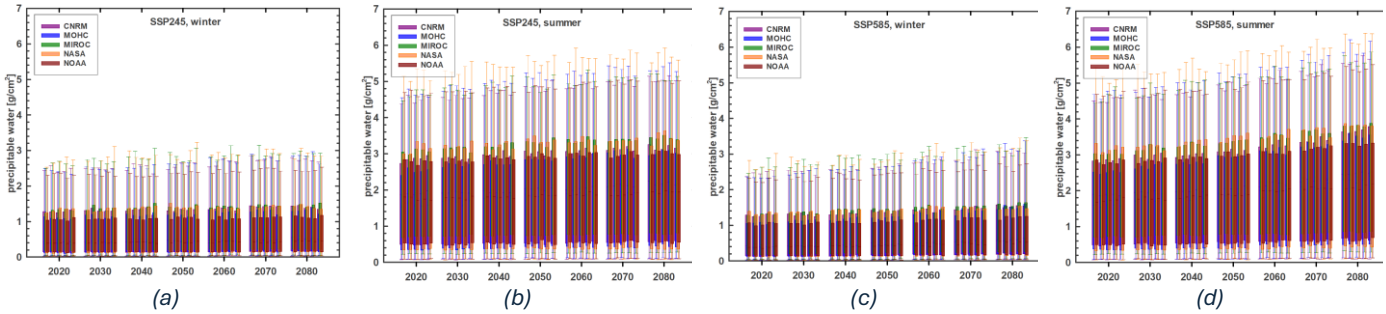

Figure 3. Precipitable water under SSP245 winter (a) & summer (b) and SSP585 winter (c) & summer (d). Winter/summer correspond to months 12-2/6-8 in the northern hemisphere and 6-8/12-2 in the southern hemisphere. Bars are for the 25th to 75th percentiles; whiskers show the 5th to 95th percentiles.

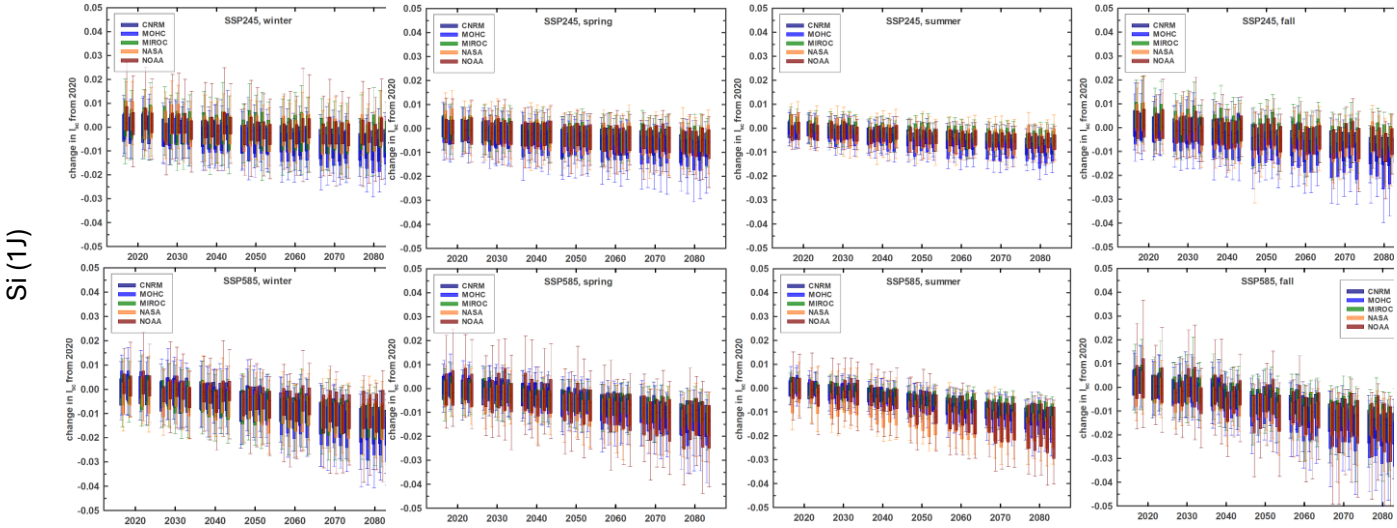

Figure 4. With aerosols held at 2020 levels, the decadal projections of the change in seasonal short-circuit current of silicon (Si) solar cells from 2020 values. Data is normalized to the relative irradiances.

Decadal forecasts: effect of water vapor

The ability of solar PV to slow destabilization of the climate will itself be altered as atmospheric changes take effect. Increases in global surface temperatures increase evaporation and the precipitable water content in the column of atmosphere above the surface[59]. The decrease in stability that results from thermal energy accumulating in the atmospheric system is expected to lead to changes in magnitude and larger fluctuations. Absorption of radiation by water vapor occurs at wavelengths both within and beyond the absorption bands of solar cells, so the proportional impact on their outputs differs from what might be found from analysis of broadband solar irradiance alone. For example, the number of photons in the standard spectrum (250-4000 nm, precipitable water=1.42 g/cm^2), is about 22% lower than that of a spectrum in an arid atmosphere (precipitable water=0 g/cm^2), Figure 1(a). The relative decrease in photons within the absorption range of silicon solar cells (~300-1200 nm) is less: about 10%. Precipitable water vapor increases with temperature, so the forecast downward trends in cell current over time shown in Figure 4 are expected from this component of anthropogenic climate change[60]. Similar decreases in solar cell current, due (primarily) to increases in water vapor, are seen with 2-junction and 3-junction cells (supplemental materials, Figure 12).

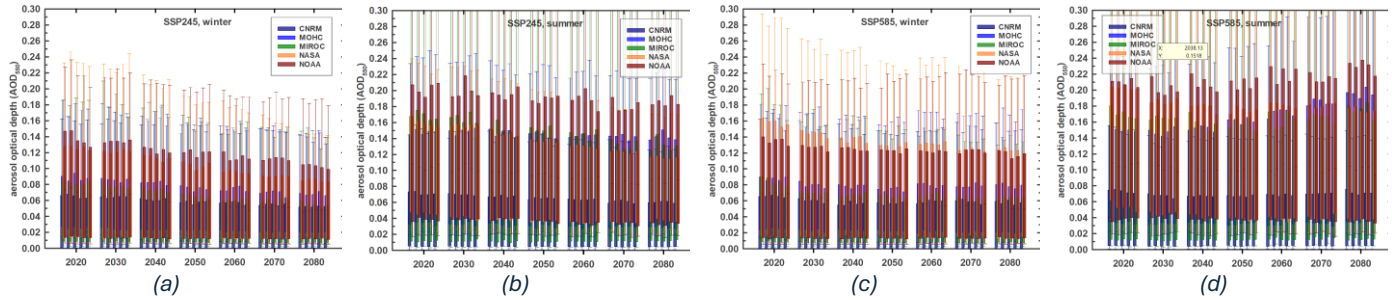

Figure 5. Aerosol optical depth at 550 nm (AOD_{550}) under SSP245 winter (a) & summer (b) and SSP585 winter (c) & summer (d). Winter/summer correspond to months 12-2/6-8 in the northern hemisphere and 6-8/12-2 in the southern hemisphere.

Decadal forecasts: water vapor and aerosols combined

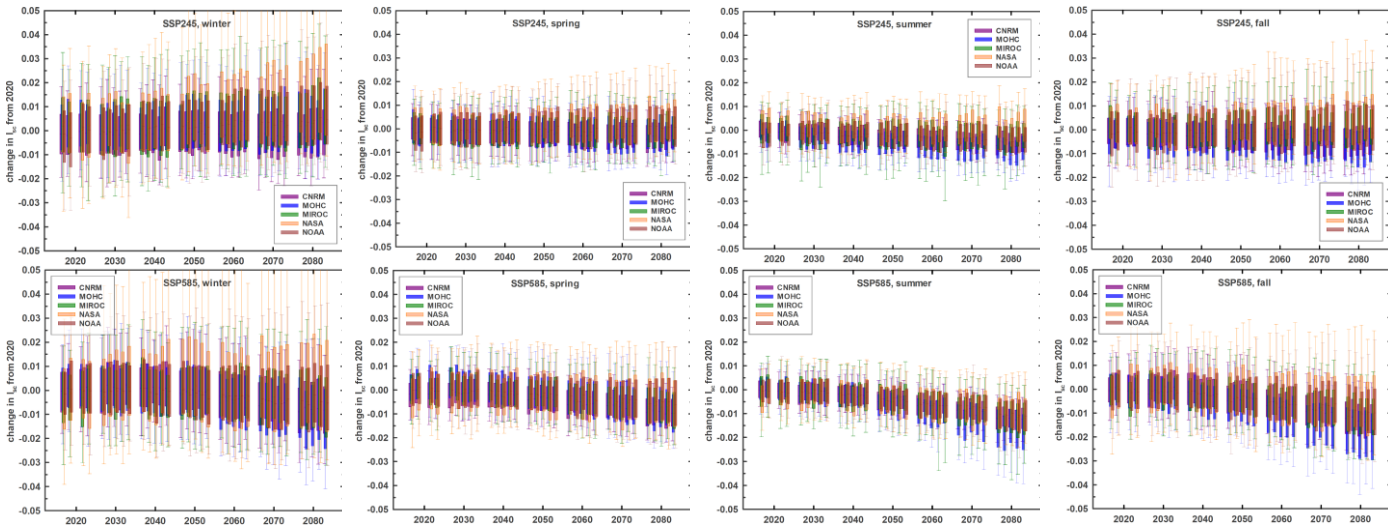

Figure 6. Decadal projections of the change in seasonal short-circuit current of single-junction (1J) silicon solar cells relative to 2020 values. Data is for latitudes below +/-60° (inclusive) and is normalized by the relative irradiance.

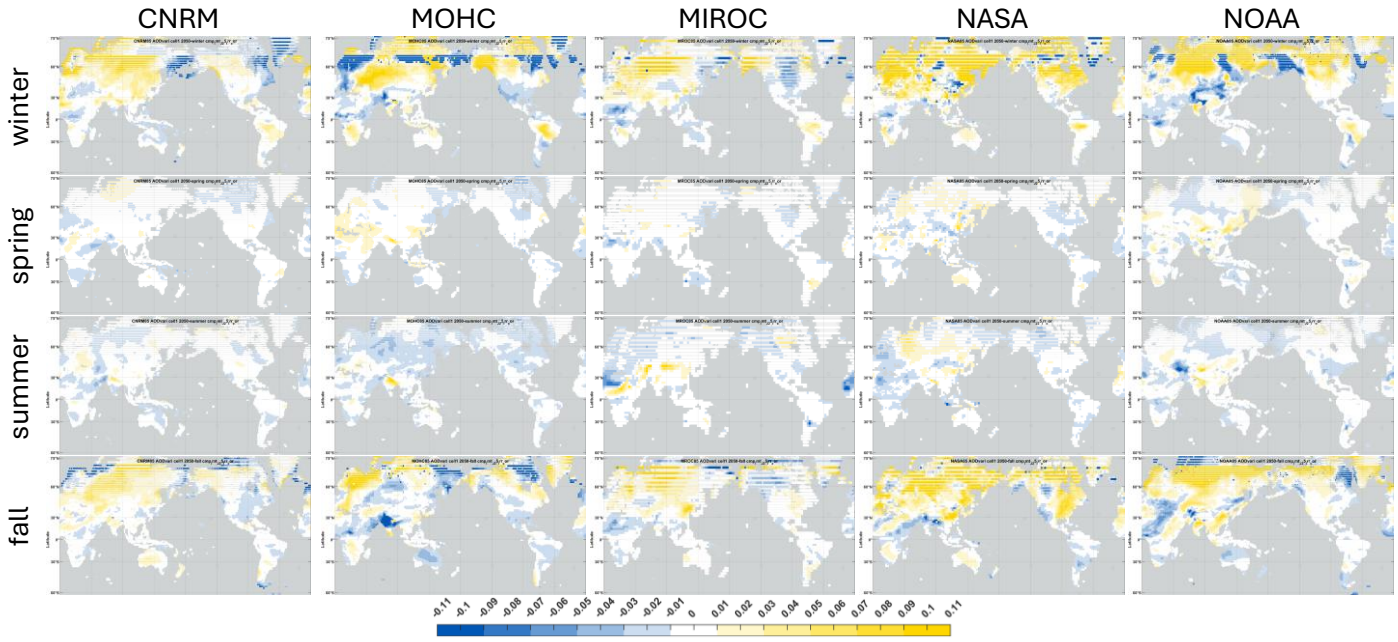

Figure 7. Silicon (1J) short-circuit current in 2050, relative to 2020 (SSP585). (The step change seen at high latitudes in winter is due to a drop in the number of months averaged (from three to two), when the sun dips below the horizon in the remaining month.)

Whereas the effect of water vapor on spectral irradiance is confined to water absorption bands (Figure 1a), the absorption and scattering from aerosols is more broadband; it depends on the size (for soot and dust) and (for molecular scattering) the chemical composition of the particles. The wavelength dependence therefore spans the spectrum of interest for solar cells and crops (Figure 1b). Aerosol levels in the atmosphere (quantified as aerosol optical depth, AOD) rise and fall due to human activity, air quality remediation, and climate change feedbacks, so are more difficult to forecast. A patchwork approach to decarbonization globally will give rise to fluctuations in aerosol levels locally and over time. Potential attempts at atmospheric geoengineering would add

to the uncertainty[61]. While the transition from coal to natural gas to zero-carbon sources reduces the aerosols emitted per unit of energy, this may prove to be more than offset by growth in total combustion worldwide. As climate zones shift, large-scale wildfires (in forests and peat bogs) may further accelerate as permafrost thaws[62] and as some of today's forest areas will no longer receive sufficient moisture to support them[63]. Conversely, decreases in aerosols are expected from climate-change-driven reductions in wind speeds[10]. The variation in model decadal forecasts for aerosol optical depth in Figure 5 reflects this uncertainty.

Figure 6 and Figure 7 incorporate the variation of aerosols into the forecast for solar cell short circuit currents. Where a net decrease in aerosols is predicted, "solar brightening" occurs and the downward trends seen in Figure 4 are reduced or, in some instances, reversed. Net spectrum-driven decreases in PV output seen due to increased water vapor could thus be avoided in cases where substantial decreases in aerosols are also obtained.

Effect on crop photosynthesis

For crop plants, analogous to the quantum efficiency of solar cells is the "spectrum of quantum yield of photosynthesis"[4]. Integrating across the "action spectrum" (the range of wavelengths that drive photosynthesis reactions) gives the quantum yield, a measure of the efficiency at which photon energy is absorbed and converted to chemical energy via fixation of carbon. Figure 1(b) shows normalized spectra of quantum yields for three commercial crops[4]. The absorption of plant pigments such as chlorophylls and carotenoids cuts off above ~700 nm, so is largely unaffected by the variations in atmospheric water vapor shown to affect solar photovoltaics.

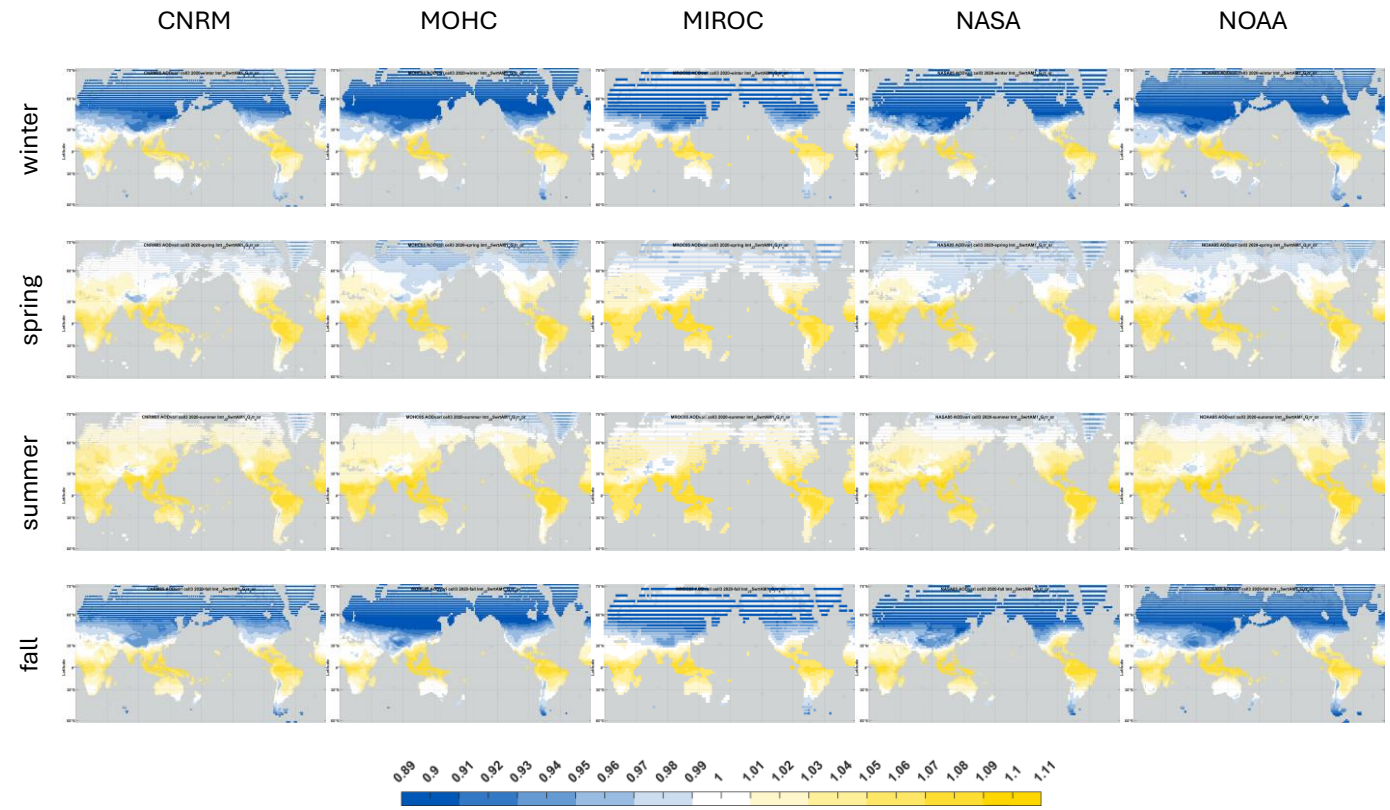

Figure 8. Predicted 2020 quantum yield of photosynthesis for maize, relative to that under the standard spectrum for photovoltaics (AM1.5G), for scenario SSP585. Data is normalized to 1000 W/m^2 irradiance. "Winter"/"spring" and "summer"/"fall" correspond to months 12-2/3-5 and 6-8/9-11 in the northern hemisphere and 6-8/9-11 and 12-2/3-5 in the southern hemisphere.

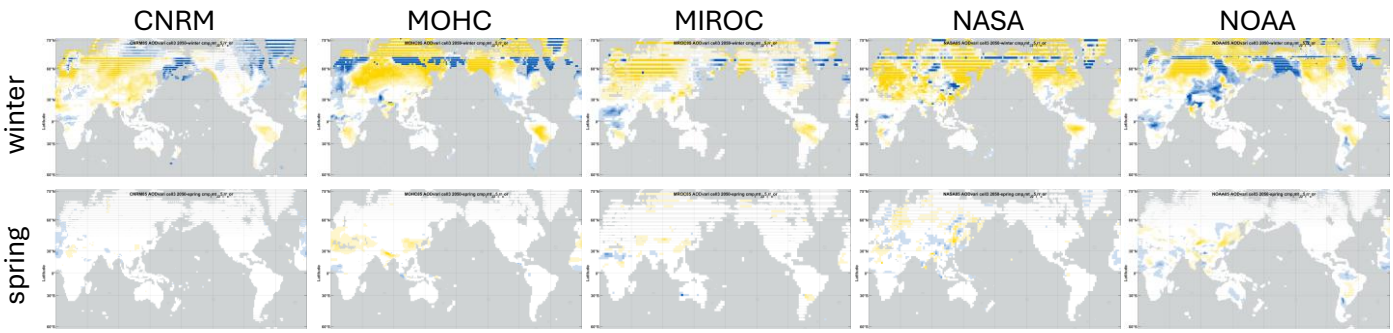

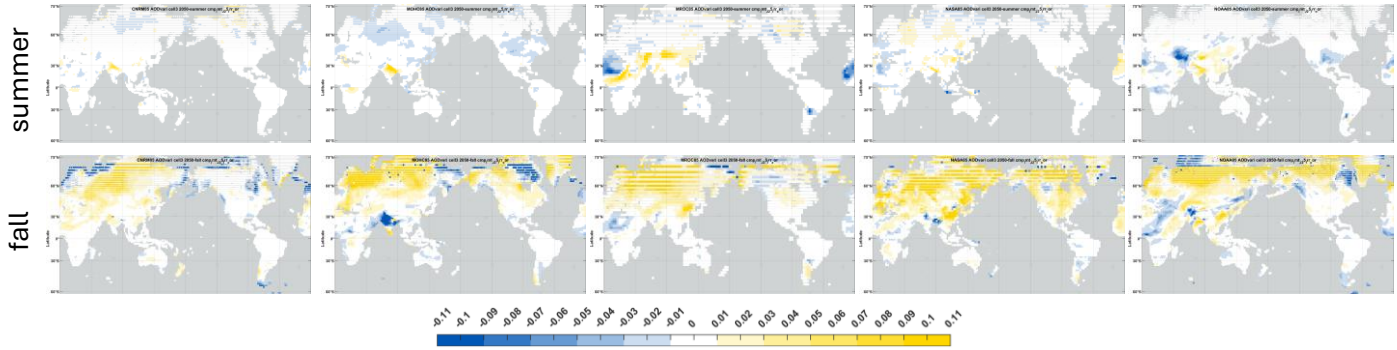

Figure 9. Maize quantum yield of photosynthesis in 2050, relative to 2020, scenario SSP585. (The step change seen at high latitudes in winter is due to a reduction in the number of months averaged (from three to two), when the sun falls below the horizon.)

Borrowing the concept of a standard spectrum from PV allows for comparison of the effect of spectrum variation on the rate of photosynthesis globally (Figure 8). For the baseline year of 2020, the global spectra are more favorable worldwide in the spring and summer, and year-round in the southern hemisphere. Given that corn, rice, and wheat are estimated to provide 60% of the food calories consumed globally, a 1% gain/loss in crop yields from this spectrum variation would correspond to the annual calorie intake of Canada. After normalizing to the broadband irradiance, the quantum yield for maize remains ~5-10% higher for much of the southern hemisphere in the spring and summer (the peak growing seasons).

The change in quantum yield of photosynthesis for maize in 2050, relative to 2020, is shown in Figure 9. The results for wheat and rice are substantially similar; their results are included in the Supplemental Materials (Figure 17 & Figure 18). Aerosol levels are projected to mostly decrease in fall and winter (Figure 5), leading to increases in the quantum yield of photosynthesis over much of the globe during these seasons. For the peak growing seasons of spring and summer, changes are more modest.

Conclusion

CMIP climate models provide a forecast for the impact of solar spectrum shifts on photovoltaic and crop production. In the decades ahead, changes in the levels of greenhouse gases and aerosols in the atmosphere will alter the sunlight spectra that reach the surface, thereby altering solar PV performance and crop photosynthesis. Future atmospheric water vapor levels will be higher and more variable, resulting in lower, more erratic photovoltaic energy output. The spectrum used in photosynthesis in corn, wheat, and rice lies largely outside the water absorption bands, so it is relatively unaffected by the changes in atmospheric water vapor. Sustained declines in fossil fuel combustion will deliver not only a reduction in greenhouse gases, but an additional dividend in reduced aerosols that will boost the spectrum of sunlight available for crop photosynthesis and photovoltaics.

Supplemental Materials

Data repository for spectra: DOI 10.5281/zenodo.18173507

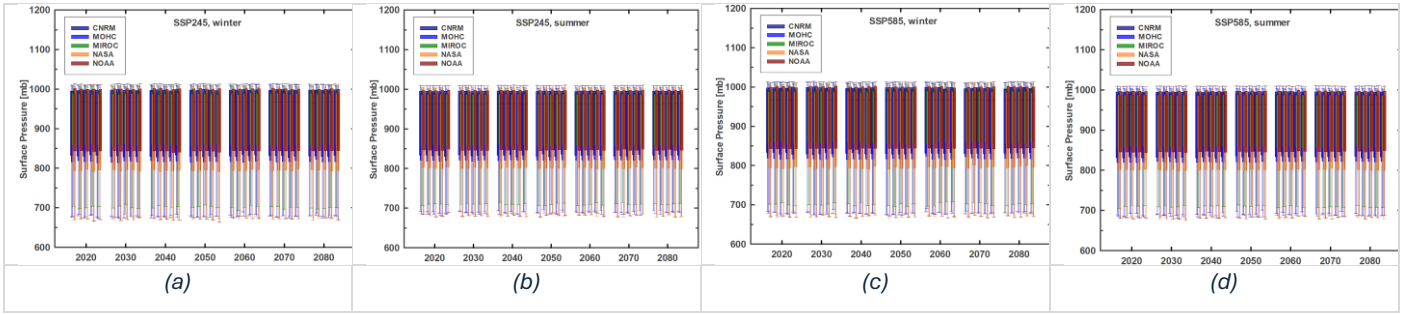

Figure 10. Surface atmospheric pressure under SSP245 winter (a) & summer (b) and SSP585 winter (c) & summer (d). Winter/summer correspond to months 12-2/6-8 in the northern hemisphere and 6-8/12-2 in the southern hemisphere.

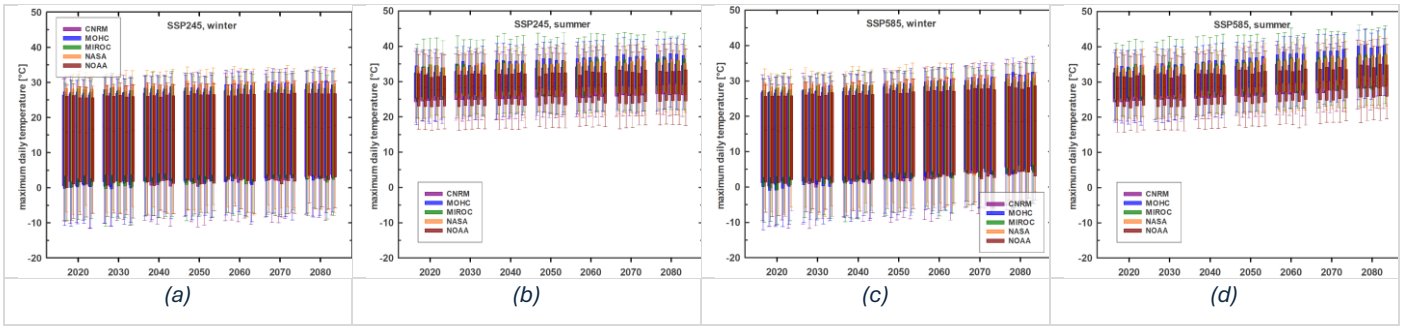

Figure 11. Maximum daily temperature under SSP245 winter (a) & summer (b) and SSP585 winter (c) & summer (d), for latitudes up to and including +/-60°. Winter/summer correspond to months 12-2/6-8 in the northern hemisphere and 6-8/12-2 in the southern hemisphere.

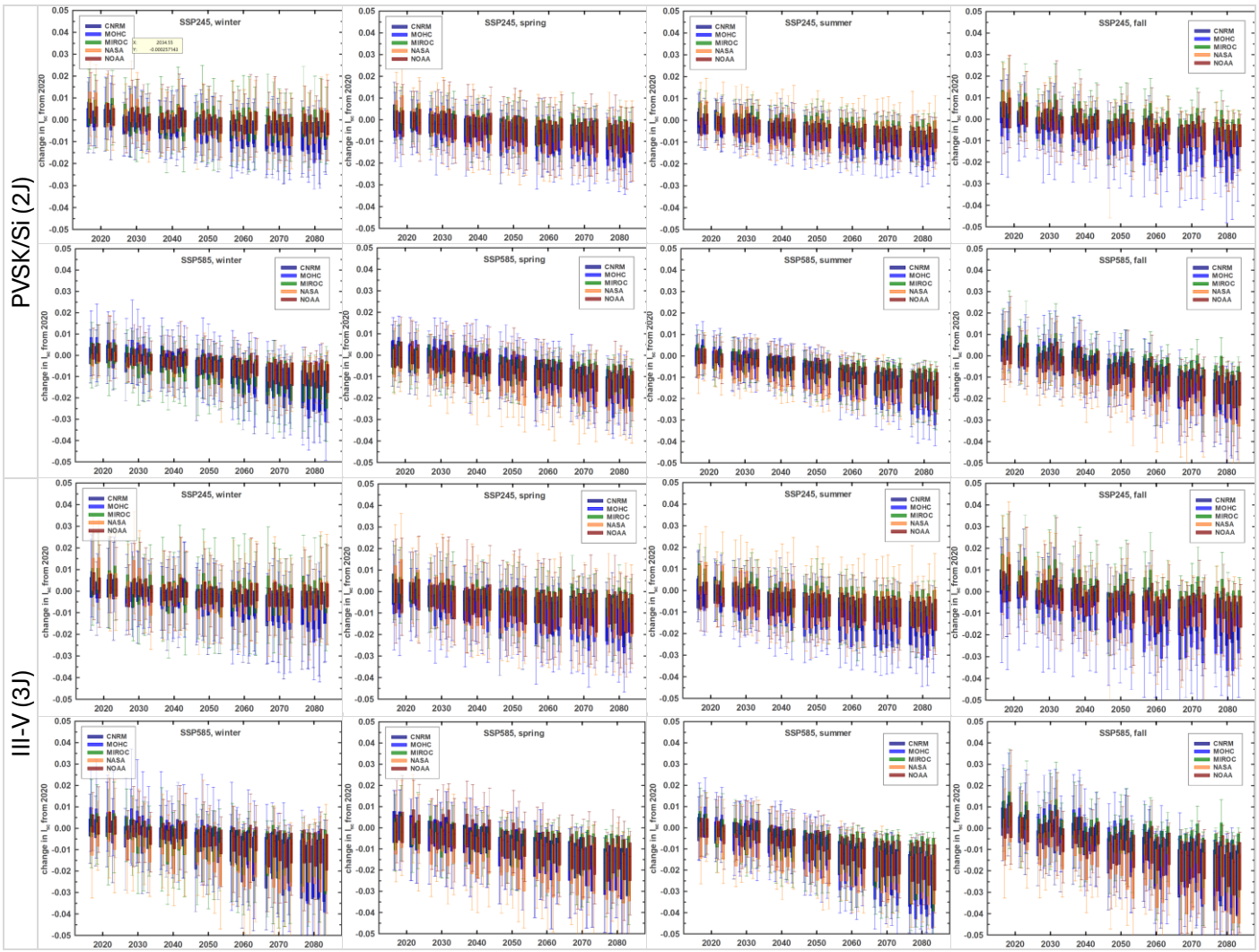

Figure 12. Decadal projections of the change in seasonal short-circuit current of tandem (2J) perovskite-silicon (PVSK/Si) and three-junction (3J) III-V multijunction (III-V) solar cells relative to 2020 values: aerosol optical depth is held constant at 2020 values. Data is normalized by the relative irradiances.

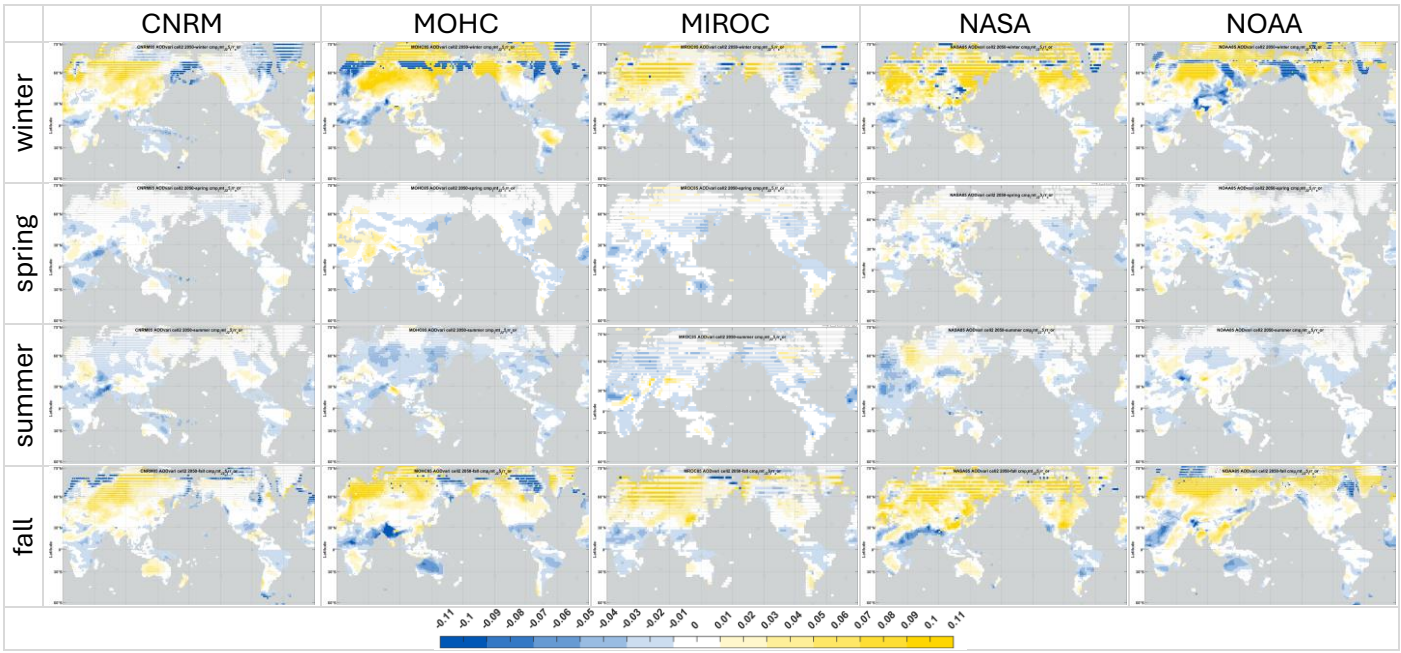

Figure 13. PVSK/Si (2J) short-circuit current in 2050, relative to 2020 (SSP585). (The step change seen at high latitudes in winter is due to a reduction in the number of months averaged (from three to two), when the sun falls below the horizon.)

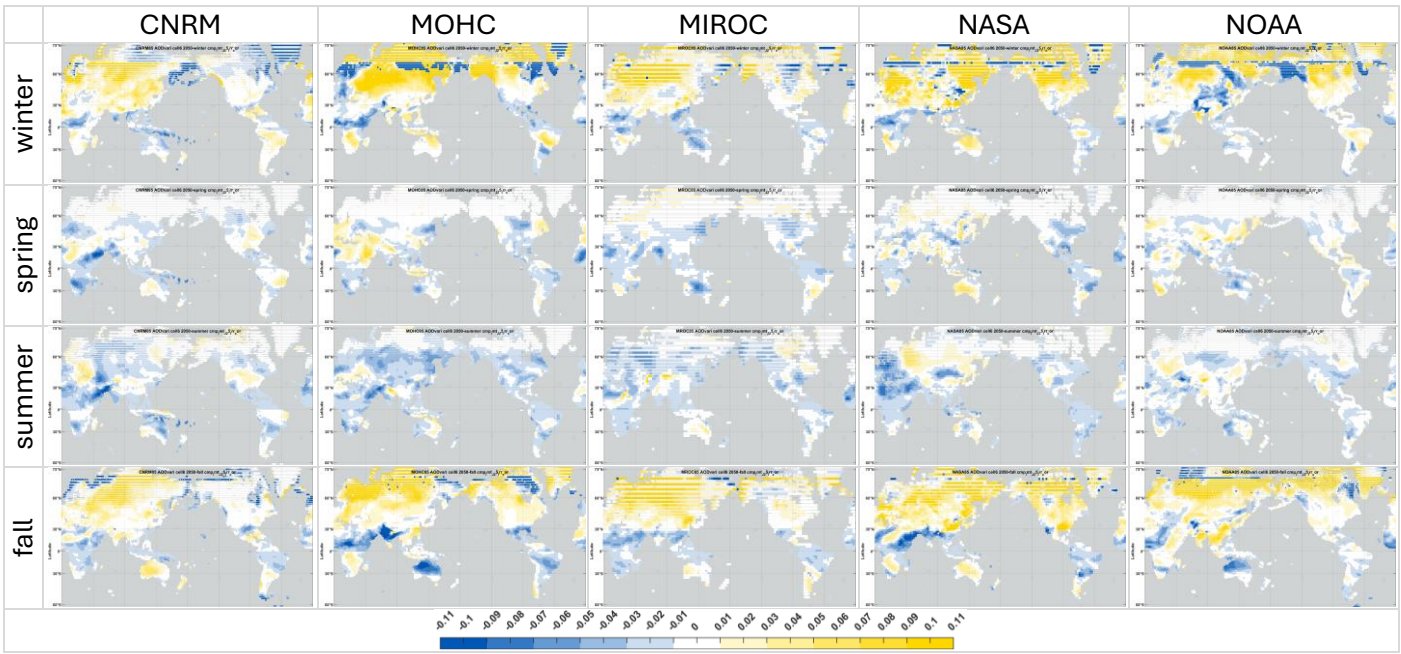

Figure 14. III-V (3J) short-circuit current in 2050, relative to 2020 (SSP585). (The step change seen at high latitudes in winter is due to a reduction in the number of months averaged (from three to two), when the sun falls below the horizon.)

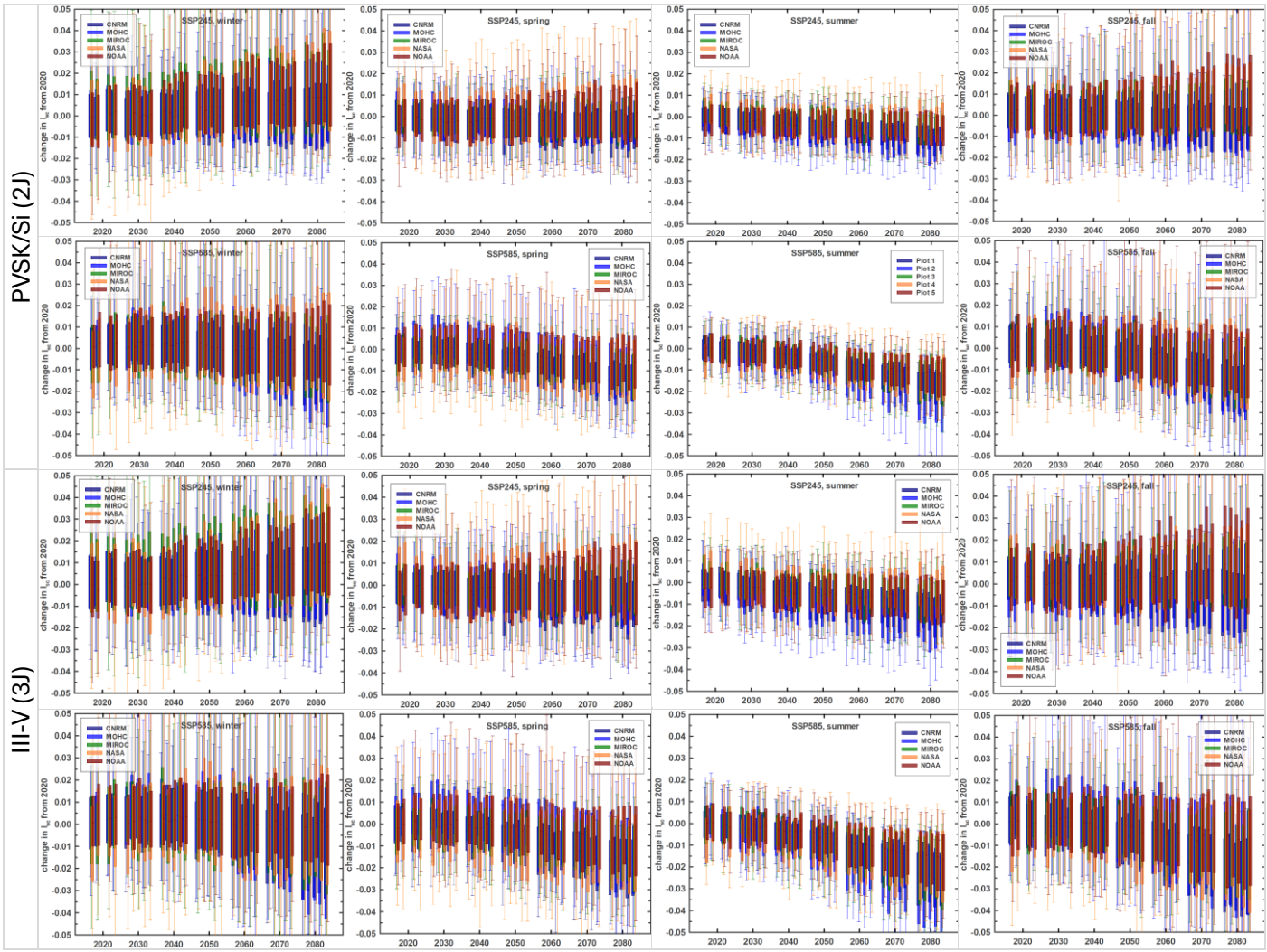

Figure 15. Decadal projections of the change in seasonal short-circuit current of perovskite/silicon (2J) and III-V (3J) solar cells relative to 2020 values. Data is normalized by the relative irradiance.

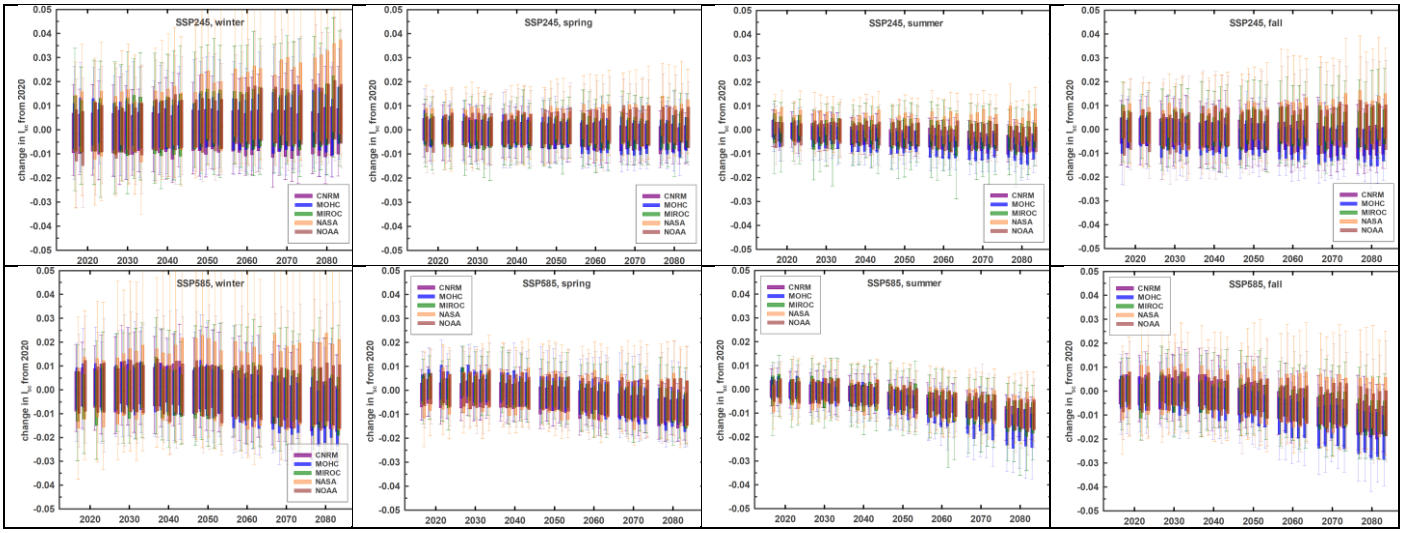

Figure 16. Decadal projections of the change in seasonal short-circuit current of single-junction (1J) silicon solar cells relative to 2020 values, but without normalization of irradiance. Data is for latitudes below +/-60° (inclusive).

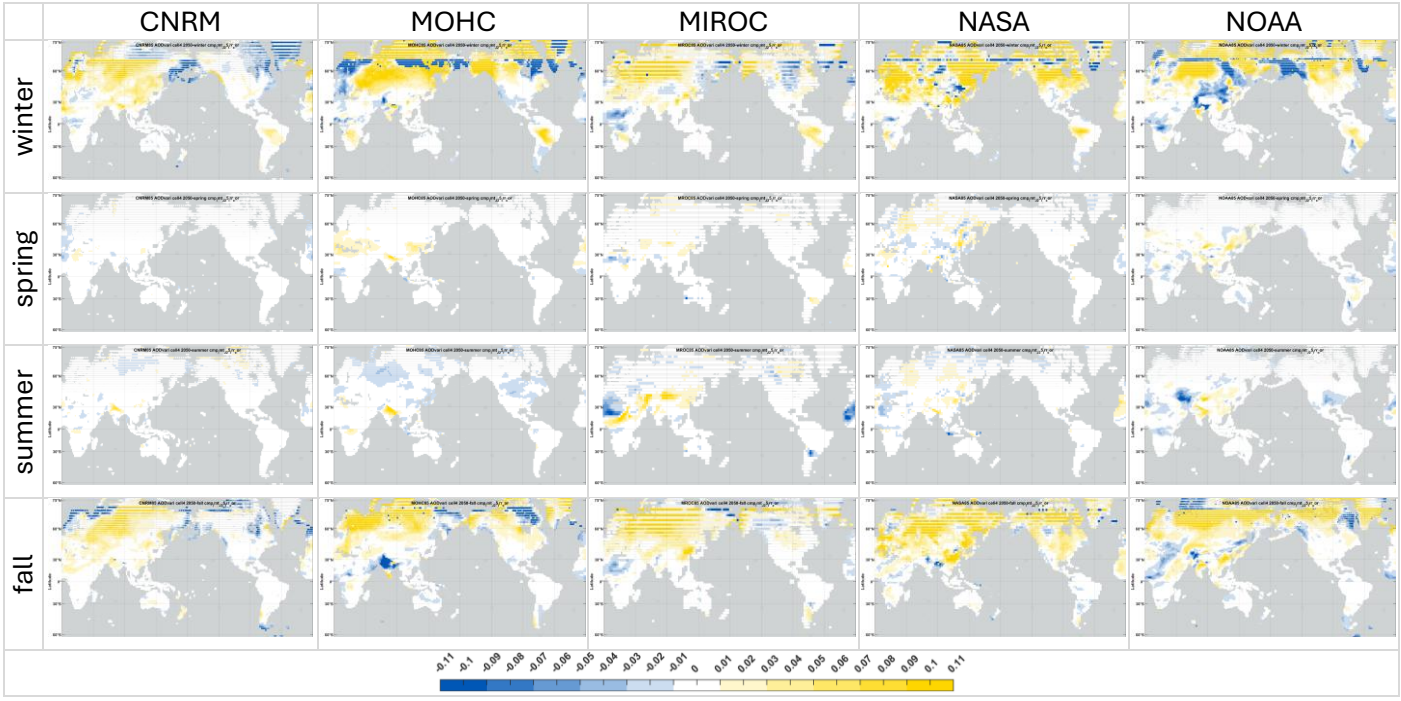

Figure 17. Wheat quantum yield of photosynthesis in 2050, relative to 2020, scenario SSP585. (The step change seen at high latitudes in winter is due to a reduction in the number of months averaged (from three to two), when the sun falls below the horizon.)

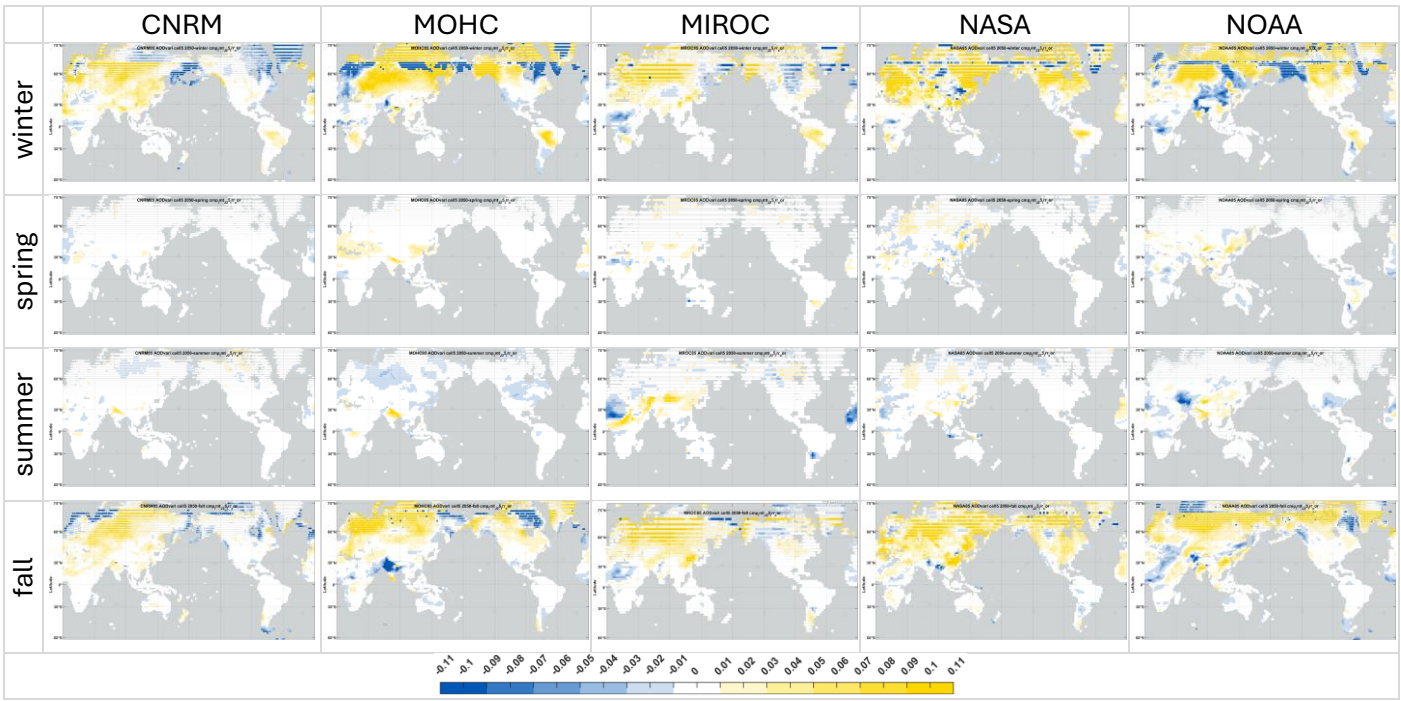

Figure 18. Rice quantum yield of photosynthesis in 2050, relative to 2020, scenario SSP585. (The step change seen at high latitudes in winter is due to a reduction in the number of months averaged (from three to two), when the sun falls below the horizon.)

References

1. Green, M. A. *et al*. Solar cell efficiency tables (version 59). *Progress in Photovoltaics: Research and Applications* 30, 3–12 (2022).
2. Green, M. A. *et al*. Solar cell efficiency tables (Version 61). *Progress in Photovoltaics: Research and Applications* 31, 3–16 (2023).
3. Green, M. A. *et al*. Solar cell efficiency tables (Version 63). *Progress in Photovoltaics: Research and Applications* 32, 3–13 (2024).
4. McCree, K. J. The action spectrum, absorptance and quantum yield of photosynthesis in crop plants. *Agricultural Meteorology* 9, 191–216 (1971).
5. Young, A. Rayleigh scattering. *Phys Today* 35, 42–48 (1982).
6. Foote, E. Circumstances affecting the heat of the Sun's rays: Art. XXXI. *The American Journal of Science and Arts* 382–383 https://ia800802.us.archive.org/4/items/mobot31753002152491/mobot31753002152491.pdf (1856).
7. Ripple, W. J. *et al*. Many risky feedback loops amplify the need for climate action. *One Earth* 6, 86–91 (2023).
8. Gillett, N. P., Zwiers, F. W., Weaver, A. J. & Stott, P. A. Detection of human influence on sea-level pressure. *Nature 2003 422:6929* 422, 292–294 (2003).
9. Overview and key findings – World Energy Outlook 2025 – Analysis - IEA. https://www.iea.org/reports/world-energy-outlook-2025/overview-and-key-findings.
10. Ren, D. Effects of global warming on wind energy availability. *Journal of Renewable and Sustainable Energy* 2, (2010).
11. Subba, T., Gogoi, M. M., Pathak, B., Bhuyan, P. K. & Babu, S. S. Recent trend in the global distribution of aerosol direct radiative forcing from satellite measurements. *Atmospheric Science Letters* 21, e975 (2020).
12. Le Treut, H. *et al*. Historical Overview of Climate Change Science Coordinating Lead Authors: Lead Authors: Contributing Authors: This chapter should be cited as. (2007).
13. Arrhenius, S. On the Influence of Carbonic Acid in the Air upon the Temperature of the Ground. *Philosophical Magazine and Journal of Science Series* 5, 237–276 (1896).
14. Edwards, P. N. History of climate modeling. *Ltd. WIREs Clim Change* 2, 128–139 (2010).
15. CMIP6: the next generation of climate models explained - Carbon Brief. https://www.carbonbrief.org/cmip6-the-next-generation-of-climate-models-explained/.
16. Intergovernmental Panel on Climate Change (IPCC). Synthesis Report — IPCC. https://www.ipcc.ch/ar6-syr/.
17. Pan, Z., Segal, M., Arritt, R. W. & Takle, E. S. On the potential change in solar radiation over the US due to increases of atmospheric greenhouse gases. *Renew Energy* 29, 1923–1928 (2004).
18. Bartók, B. Changes in solar energy availability for south-eastern Europe with respect to global warming. *Physics and Chemistry of the Earth, Parts A/B/C* 35, 63–69 (2010).
19. Jerez, S. *et al*. The impact of climate change on photovoltaic power generation in Europe. *Nature Communications 2015 6:1* 6, 1–8 (2015).
20. Schaeffer, R. *et al*. Energy sector vulnerability to climate change: A review. *Energy* 38, 1–12 (2012).
21. Gaetani, M. *et al*. The near future availability of photovoltaic energy in Europe and Africa in climate-aerosol modeling experiments. *Renewable and Sustainable Energy Reviews* 38, 706–716 (2014).
22. Bloomfield, H. C. *et al*. Quantifying the sensitivity of european power systems to energy scenarios and climate change projections. *Renew Energy* 164, 1062–1075 (2021).

23. Gernaat, D. E. H. J. *et al.* Climate change impacts on renewable energy supply. *Nat Clim Chang* 11, 119–125 (2021).

24. Jaxa-Rozen, M. & Trutnevyte, E. Sources of uncertainty in long-term global scenarios of solar photovoltaic technology. *Nat Clim Chang* 11, 266–273 (2021).

25. Feron, S., Cordero, R. R., Damiani, A. & Jackson, R. B. Climate change extremes and photovoltaic power output. *Nat Sustain* 4, 270–276 (2021).

26. Yin, J., Molini, A. & Porporato, A. Impacts of solar intermittency on future photovoltaic reliability. *Nature Communications 2020 11:1* 11, 1–9 (2020).

27. Kozarcanin, S., Liu, H. & Andresen, G. B. 21st Century Climate Change Impacts on Key Properties of a Large-Scale Renewable-Based Electricity System. *Joule* 3, 992–1005 (2019).

28. Ohunakin, O. S., Adaramola, M. S., Oyewola, O. M., Matthew, O. J. & Fagbenle, R. O. The effect of climate change on solar radiation in Nigeria. *Solar Energy* 116, 272–286 (2015).

29. Huber, I. *et al.* Do climate models project changes in solar resources? *Solar Energy* 129, 65–84 (2016).

30. Burnett, D., Barbour, E. & Harrison, G. P. The UK solar energy resource and the impact of climate change. *Renew Energy* 71, 333–343 (2014).

31. Panagea, I. S., Tsanis, I. K., Koutroulis, A. G. & Grillakis, M. G. Climate change impact on photovoltaic energy output: The case of Greece. *Advances in Meteorology* 2014, (2014).

32. Ghanim, M. S. & Farhan, A. A. Projected patterns of climate change impact on photovoltaic energy potential: A case study of Iraq. *Renew Energy* 204, 338–346 (2023).

33. Crook, J. A., Jones, L. A., Forster, P. M. & Crook, R. Climate change impacts on future photovoltaic and concentrated solar power energy systems. *Energy Environ Sci* 4, 3101–3109 (2011).

34. Patt, A., Pfenninger, S. & Lilliestam, J. Vulnerability of solar energy infrastructure and output to climate change. *Clim Change* 121, 93–102 (2013).

35. Pašičko, R., Branković, Č. & Šimić, Z. Assessment of climate change impacts on energy generation from renewable sources in Croatia. *Renew Energy* 46, 224–231 (2012).

36. Müller, J., Folini, D., Wild, M. & Pfenninger, S. CMIP-5 models project photovoltaics are a no-regrets investment in Europe irrespective of climate change. *Energy* 171, 135–148 (2019).

37. Kinsey, G. S. Impact of climate change on PV power production. *Spectral Characteristics of Solar Radiation: Applications in Photovoltaic Conversion* 455–483 (2025) doi:10.1016/B978-0-443-23839-0.00016-X.

38. Simkin, A. J., López-Calcagno, P. E., Raines, C. A. & Lunn, J. E. Feeding the world: improving photosynthetic efficiency for sustainable crop production. *J Exp Bot* 70, 1119–1140 (2019).

39. SHAFIQ, I. *et al.* Crop photosynthetic response to light quality and light intensity. *J Integr Agric* 20, 4–23 (2021).

40. Guo, X. *et al.* Effects of LEDs Light Spectra on the Growth, Yield, and Quality of Winter Wheat (Triticum aestivum L.) Cultured in Plant Factory. *J Plant Growth Regul* 42, 2530–2544 (2023).

41. Ouzounis, T., Rosenqvist, E. & Ottosen, C. O. Spectral effects of artificial light on plant physiology and secondary metabolism: A review. *HortScience* 50, 1128–1135 (2015).

42. Gueymard, C. A. The SMARTS spectral irradiance model after 25 years: New developments and validation of reference spectra. *Solar Energy* 187, 233–253 (2019).

43. Voldoire, A. CNRM-CERFACS CNRM-ESM2-1 model output prepared for CMIP6 ScenarioMIP ssp585. Preprint at https://doi.org/https://doi.org/10.22033/ESGF/CMIP6.4226 (2023).

44. Voldoire, A. CNRM-CERFACS CNRM-ESM2-1 model output prepared for CMIP6 ScenarioMIP ssp245. Preprint at https://doi.org/https://doi.org/10.22033/ESGF/CMIP6.4191 (2023).

45. Good, P. *et al.* MOHC UKESM1.0-LL model output prepared for CMIP6 ScenarioMIP ssp585. Preprint at https://doi.org/10.22033/ESGF/CMIP6.6405 (2019).

46. Good, P. *et al.* MOHC UKESM1.0-LL model output prepared for CMIP6 ScenarioMIP ssp245. Preprint at https://doi.org/10.22033/ESGF/CMIP6.6339 (2019).

47. Kinsey, G. S. Solar cell efficiency divergence due to operating spectrum variation. *Solar Energy* 217, 49–57 (2021).

48. Kinsey, G. S. Spectrum sensitivity, energy yield, and revenue prediction of PV modules. *IEEE J Photovolt* https://doi.org/10.1109/JPHOTOV.2014.2370256 (2015) doi:10.1109/JPHOTOV.2014.2370256.

49. Kinsey, G. S., Nayak, A., Liu, M. & Garboushian, V. Increasing power and energy in Amonix CPV solar power plants. *IEEE J Photovolt* 1, (2011).

50. Kinsey, G. S. *et al.* Impact of measured spectrum variation on solar photovoltaic efficiencies worldwide. *Renew Energy* https://doi.org/10.1016/J.RENENE.2022.07.011 (2022) doi:10.1016/J.RENENE.2022.07.011.

51. Snapshot 2021 - IEA-PVPS. https://iea-pvps.org/snapshot-reports/snapshot-2021/.

52. Electricity consumption by country, around the world | TheGlobalEconomy.com. https://www.theglobaleconomy.com/rankings/electricity_consumption/.

53. Chen, B. & Liu, Z. Global water vapor variability and trend from the latest 36 year (1979 to 2014) data of ECMWF and NCEP reanalyses, radiosonde, GPS, and microwave satellite. *Journal of Geophysical Research: Atmospheres* 121, 11,442-11,462 (2016).

54. Ren, D., Wang, Y., Wang, G. & Liu, L. Rising trends of global precipitable water vapor and its correlation with flood frequency. *Geod Geodyn* 14, 355–367 (2023).

55. A startup says it's begun releasing particles in the atmosphere, in an effort to tweak the climate | MIT Technology Review. https://www.technologyreview.com/2022/12/24/1066041/a-startup-says-its-begun-releasing-particles-into-the-atmosphere-in-an-effort-to-tweak-the-climate/.

56. Kim, I. W. *et al.* Abrupt increase in Arctic-Subarctic wildfires caused by future permafrost thaw. *Nature Communications 2024 15:1* 15, 1–11 (2024).

57. Barkhordarian, A., Saatchi, S. S., Behrangi, A., Loikith, P. C. & Mechoso, C. R. A Recent Systematic Increase in Vapor Pressure Deficit over Tropical South America. *Scientific Reports 2019 9:1* 9, 1–12 (2019).